

# CHANGE VISUALIZATION THROUGH A TEXTURE-BASED ANALYSIS APPROACH FOR DISASTER APPLICATIONS

D. Tomowski<sup>a,\*</sup>, S. Klonus<sup>a</sup>, M. Ehlers<sup>a</sup>, U. Michel<sup>b</sup>, P. Reinartz<sup>c</sup>

<sup>a</sup> Institute for Geoinformatics and Remote Sensing, University of Osnabrueck, 49076 Osnabrueck, Germany -  
(dtomowski, sklonus, mehlers)@igf.uni-osnabrueck.de

<sup>b</sup> University of Education, Department of Geography, Heidelberg, Germany (e-mail: michel@ph-heidelberg.de)

<sup>c</sup> German Aerospace Center DLR, Remote Sensing Technology Institute, Wessling, Germany -  
peter.reinartz@dlr.de

**KEY WORDS:** Change Detection, Comparison, Visualization, Disaster, Texture

## ABSTRACT:

A fast detection and visualization of change in crisis areas is an important condition for planning and coordination of help. The availability of new satellites with high temporal resolution (e.g. RapidEye) and/or high spatial resolution (e.g. Quickbird) provides the basis for a better visualization of multitemporal change. For automated change detection, a large number of algorithms has been proposed and developed. This article describes the results of four texture based change detection approaches that were applied to satellite images of the Darfur crisis region. In our methodology we calculate firstly different texture characteristics ("energy", "correlation", "contrast" and "inverse distance moment"), for a whole image at two (or more) different times. The second step is to test the capability of known change detection methods (image-differencing, image-ratioing, regression analysis and principal component analysis) to visualize the change of settlement areas through these texture characteristics and texture images, respectively. The comparison of different texture characteristics with different change detection methods shows that best results can be obtained using a selective bitemporal principal component analysis with the texture feature "energy".

## 1. INTRODUCTION

A fast detection and visualization of change in crisis areas is an important condition for planning and coordination of help (Kuenzel, 2007). Remote sensing images offer an excellent means for the rapid detection and analysis of change. Consequently, many algorithms for automated change detection have been proposed, developed, and tested. An overview and comparison of different techniques can be found, for example, in Singh (1989), Macleod and Congalton (1998), Mas (1999), Lu et al. (2003), Coppin et al. (2004), or Janyaa et al. (2008). However, a "best algorithm" for the automated detection of changes for all applications has yet to be developed if this is at all possible (Niemeyer and Nussbaum, 2006). There exist a wide range of different methods with different grades of flexibility, robustness, practicability and significance (Niemeyer and Nussbaum, 2006). These methods can be divided into three categories (Mas, 1999): Image enhancement methods, multitemporal analysis and post classification comparison. Other approaches combine these methods with each other or have a completely novel methodology.

The image enhancement methods are based on unclassified image data, which combine the data mathematically to enhance the image quality (Jensen, 1986). Examples are image-differencing, image-ratioing, principal component analysis (pca), or regression analysis.

Multitemporal analysis (Coppin et al., 2004) is based up on an isochronic analysis of multitemporal image data. This means that n bands of an image at time  $t_1$  and n bands of an image at time  $t_2$  of the same area are merged to form a new image with  $2n$  bands to extract the changed areas in this merged picture (Khorram et al., 1999).

Post classification analysis is based on a comparison of two independent classification results for at least two point of times  $t_1$  und  $t_2$ . This method allows the determination of the kind of change from one class to another class.

The high number of published scientific results in the case of combined and novel change detection methods is a clear indication of the importance of this research topic. For example, Prakash and Gupta (1998) combine the image-differencing approach with vegetations indices. Lu et al. (2005) use the image-differencing method together with a principal component analysis. Dai and Khorram (1999) employ neuronal networks whereas Foody (2001) and Nemmour and Chibani (2006) make use of fuzzy-set theory for change detection. Other approaches are based on object-based image analysis (see, for example, Im et al. 2008 or Lohmann et al. 2008).

In our approach, we use image-enhancement methods not for the spectral reflectance values but for different texture characteristics which produce a higher degree of robustness for the change detection and analysis.

## 2. THEORETICAL BACKGROUND

This section introduces the selected change detection methods for comparison and explains the calculation of the texture features.

### 2.1 Change detection methods

The first introduced method is image-differencing which is easy to understand and to implement (Singh, 1989). The method is based on calculating the grey value differences. For every pair of grey values at the same location in different points in time the difference is calculated. If the resulting values are unchanged after the algebraic subtraction or do not exceed a

---

\* Corresponding author

pre-determined threshold no change has occurred. The degree of change, on the other hand, is determined by the grey value differences. Very similar is the image-ratio method. For every pair of grey values at the same location in different points in time the ratio of the two values is calculated. Both methods vary through different combinations of spectral bands, the choice of the correct thresholds or different available spectral resolutions. Especially the choice of a correct threshold level is a critical factor (Jensen, 1986), because of a time consuming manual interpretation and the integration of a priori knowledge in the analysis process.

The regression analysis is a statistical method to determine the kind and grade of coherence of features (Mueller, 2000). The idea is to express the relation of a dependent feature to one or more independent variables. In our applied regression method of change detection, pixels from the first time are assumed to be a function of the time  $t_2$  pixel. This relation is expressed through a regression function. The type of regression function is based on the used data or a specific application. In our work we use a least squares method to calculate the regression function. After that, the predicted value ( $t_2$ ) from the regression line can be subtracted from the value in  $t_1$  to determine the change (for more details see Singh, 1989).

The principal component analysis is a statistical method to calculate new synthetic data space. With this approach, it is possible to intensify wavelength dependent material specific differences. Detailed explanations of this method can be found in Bahrenberg et al. (1992) or Schowengerdt (2007). For change detection, the principal component analysis can be used in different ways (Nussbaum and Menz, 2008). In our study, we employ a selective bitemporal PCA. This means that in a twodimensional feature space two bitemporal spectral bands of the same location are analyzed (Figure 1).

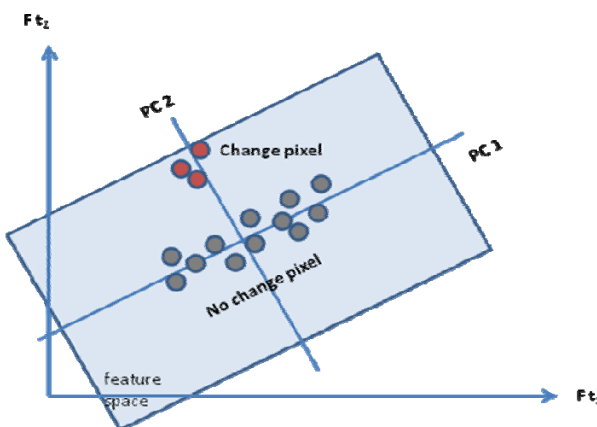


Figure 1. Change detection through bitemporal selective PCA

As result all grey values are located in relation to the principal components. The unchanged pixels have a high correlation with the first principal component in contrast to the change pixels. As a consequence, the first principal component contains the unchanged information und the second component the change information (Macleod and Congalton, 1998).

## 2.2 Calculation of texture features

The calculation of the texture features is based on the grey-level co-occurrence matrix (GLCM) (Haralick et al., 1973; Haralick

and Shapiro, 1992) which represents a second order (Sali and Wolfson, 1992).

The main idea is that settlement areas have higher texture values as non-settlement areas. Many publications of settlement analysis through remote sensing techniques prove these fact (see, for example, Myint, 2007; Steinnocher, 1997; Ehlers and Tomowski, 2008). Here, the GLCM that examine the spectral as well as the spatial distribution of grey values in the image forms the basis for the texture calculation. A GLC matrix describes the likelihood of the transition of the grey value  $i$  to the grey value  $j$  of two neighbouring pixels (Tomowski et al., 2006). During a calculation of a GLCM, the frequency of all possible grey value combinations of two neighbouring grey values with a defined displacement vector (see figure 2) for both neighbours in both directions of a specific direction ( $0^\circ$ ,  $45^\circ$ ,  $90^\circ$  or  $135^\circ$ ) can be counted.

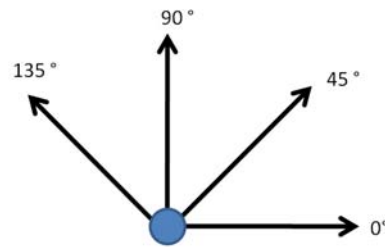


Figure 2. Possible Directions for the displacement vector

This step can be applied for four possible directions. The calculation of the average of these four matrices for every element leads to a direction independent symmetric matrix. Finally, to calculate the likelihood of a grey value transition, every value in this matrix is divided through the maximum number of all possible grey value transitions (eq. 1):

$$P_{i,j} = \frac{V_{r,c}}{\sum_{r,c=0}^{N-1} V_{r,c}} \quad (1)$$

where  $V$  = value in the symmetric GLCM  
 $r, c$  = row and column number  
 $N$  = number of rows or columns

The calculation of the GLCM with high radiometric resolution is a very time consuming step. To reduce this effect, Haralick et al. (1973) suggest different texture features which represent the texture characteristic in a single value. Based on this features new texture images can be calculated over a sliding window technique (for more details see, for example, Lehmann et al., 1997). We use the following texture features in our work:

- *Contrast* (eq. 2) is able to detect the intensity differences between a grey value of a pixel and his neighbourhood.
- *Correlation* (eq. 3) expresses the linear coherence between a grey value pixel in relation to the investigated picture and the texture feature
- *Energy* (eq. 4) calculates the sum of the squared elements in the GLCM and describes the homogeneity of the investigated picture.

- *Inverse distance moment* (IDM) (eq. 5). With the application of the IDM, it is possible to distinguish between heterogeneous and partially homogeneous non-settlement areas.

$$\sum_{i,j=0}^{N-1} P_{i,j} (i-j)^2 \quad (2)$$

$$\sum_{i,j=0}^{N-1} P_{i,j} \left[ \frac{(i-\mu_i)(j-\mu_j)}{\sqrt{(\sigma_i^2)(\sigma_j^2)}} \right] \quad (3)$$

$$\sum_{i,j=0}^{N-1} P_{i,j}^2 \quad (4)$$

$$\sum_{i,j=0}^{N-1} \frac{P_{i,j}}{1 + (i-j)^2} \quad (5)$$

where  $\mu_i = \sum_{i,j=0}^{N-1} i(P_{i,j})$   
 $\mu_j = \sum_{i,j=0}^{N-1} j(P_{i,j})$   
 $\sigma_i = \sqrt{\sum_{i,j=0}^{N-1} P_{i,j} (i - \mu_i)^2}$   
 $\sigma_j = \sqrt{\sum_{i,j=0}^{N-1} P_{i,j} (j - \mu_j)^2}$

i, j = grey values

### 3. IMPLEMENTATION

In this section we introduce our test area. After that, we explain our approach and show the results of our comparison.

#### 3.1 Test area und image data

The study area is located in Sudan. The village Shangil Tobay is located in North Darfur, and was one of seventeen villages in this region, which was attacked and destroyed since 2004 in the Darfur conflict. The conflict in Darfur is a dispute between different ethnic groups, local militia (Janjawid) and the Sudanese government. As is usual the case in these conflicts, the main suffering is sustained by the civilian population. More than 200,000 people have already died; more than 2 Million people have been displaced. The region around Shangil, a sparsely populated area, is the home of several thousands of displaced civilians. The attacks on this village took place between 2005 and 2006. To document the dimension of the inhumanities, Amnesty International (2009) and AAAS (2009) maintain web sites that shows satellite images of the affected regions before and after an attack on several villages. With the permission of the satellite company Digital Globe, we were able

to use preprocessed georeferenced Quickbird data before and after an attack for our change analysis. Figures 2 and 3 show the study area on 10 March 2003 and 18 December 2006, respectively. For our tests, we used a subset of 512 pixel \* 512 pixel with a 0,6 m ground pixel size and a radiometric resolution of 8 bit. A visual comparison and overlay of the existing man-made structures shows a high congruence between both images, so that a new co-georeferencing was not necessary and the problem of possible pseudo change was negligible. The selected subset is a village in the east of Shangil Tobay. It is visible, that the nearly the whole village was demolished; only a few buildings are not destroyed. Some of the structures were completely wiped out; some were burnt down and are still partly visible.

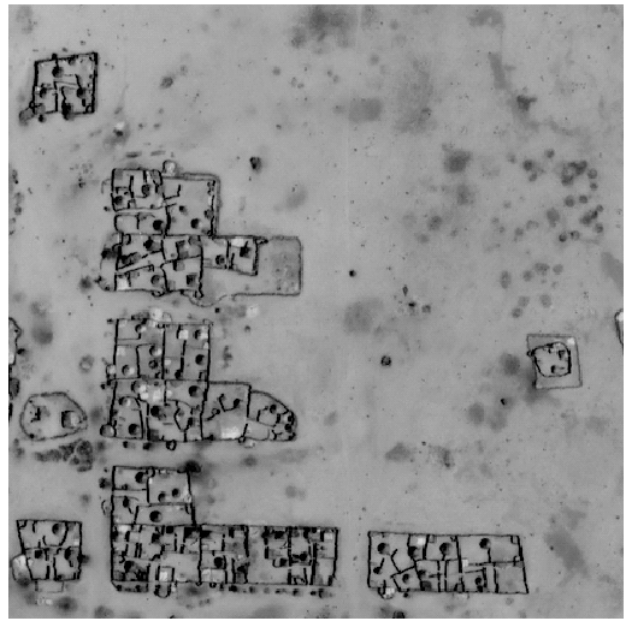


Figure 3. Subset of the Shangil village before destruction  
©Digital Globe 2003

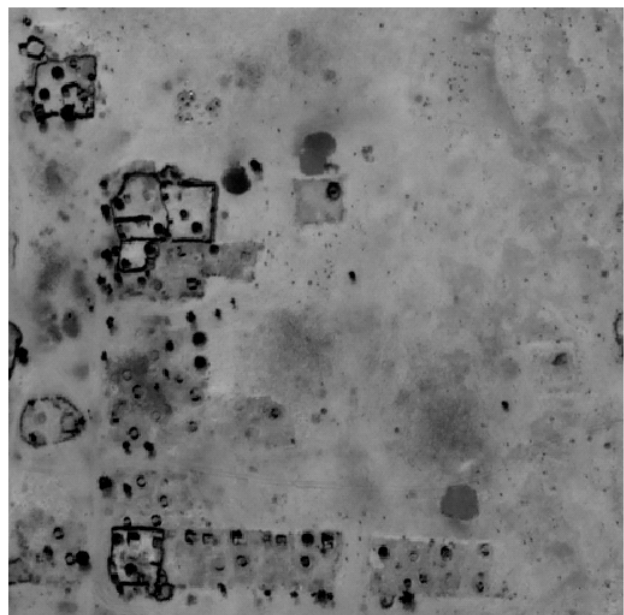


Figure 4. Subset of the Shangil village after destruction  
©Digital Globe 2006

### 3.2 Change Detection Concept and Design

Figure 5 shows the general steps that are the prerequisite for the change detection analysis. To apply our change detection methods, firstly all 3 bands (RGB) from the images taken at  $t_1$  and  $t_2$  were averaged to obtain a single band. The different texture features are calculated from the averaged data and then submitted to the different change detection analysis methods (image-differencing, image-ratioing, regression analysis and PCA). Basis for the calculation of the texture features are the images at the specified time  $t_1$  und  $t_2$ . After the texture calculation, we derived the GLCM (8 bit) for every image. Based on the GLCM we calculated the texture features *contrast*, *correlation*, *IDM* and *energy* for every point in time with differently sized windows (ranging from  $3 \times 3$ , to  $13 \times 13$  windows). Using these texture features, we then performed the four change detection methods explained above. Because of the different illumination conditions in the two images (see figure 2 and 3) we also included in a second processing step a histogram matching to both image data sets to improve the contrast and to harmonize the grey value distribution of the images (Yang and Lo, 2000).

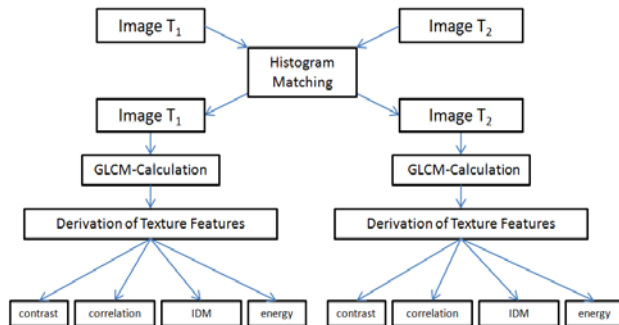


Figure 5. Steps for the derivation of texture image data for change detection

Best results were obtained using a  $13 \times 13$  window for the calculation of the texture features after the histogram matching. Again, we performed the change detection analysis four times (image-differencing, image-ratioing, regression analysis and PCA) with all derived texture images.

### 3.3 Results and interpretation

As result, we generated 16 change images (with 4 kinds of texture features and 4 change detection methods). In this paper, we will concentrate on best result and present only a short summary for the other findings. As our goal was the visualization of changes, we did not perform a quantitative accuracy analysis but concentrated on a qualitative visual interpretation (see table 8).

The image-differencing method showed the worst results for all four texture images. Therefore we will not pursue this methods in further studies.

The texture based image-ratio approach did not produce satisfying results in the case of the texture features *contrast* and *correlation*. Certainly, with the *IDM* and the *energy* feature a partial detection of change in the settlement areas is visible.

The texture based regression analysis led to partly suitable results; problems were the imprecise location of building contours. It may have some usefulness, however, in object-based image analysis.

The results for the texture based PCA with the images derived from the features *contrast*, *correlation* und *IDM* were not satisfying. However, bitemporal PCA for the texture feature *energy* proved to be the best results as far as visual appearance is concerned.

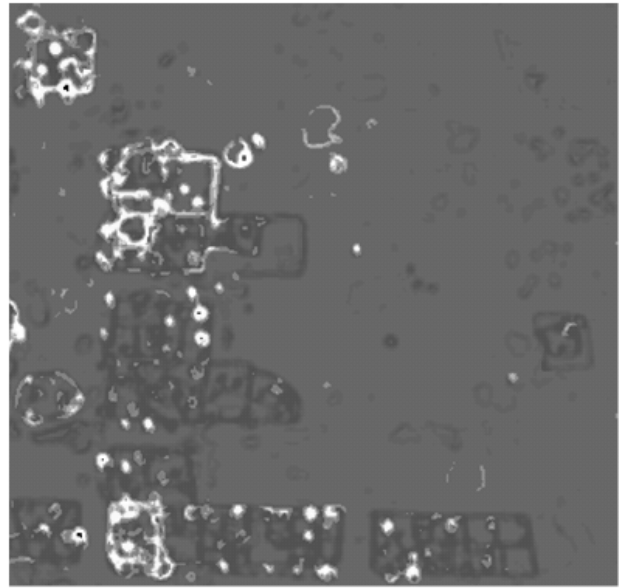


Figure 6. Results of texture based PCA with the texture feature *energy*

It is possible to visualize changed (dark grey) unchanged settlement areas (bright grey) and unchanged non-settlement-areas (medium grey) without determine thresholds (see figure 6):

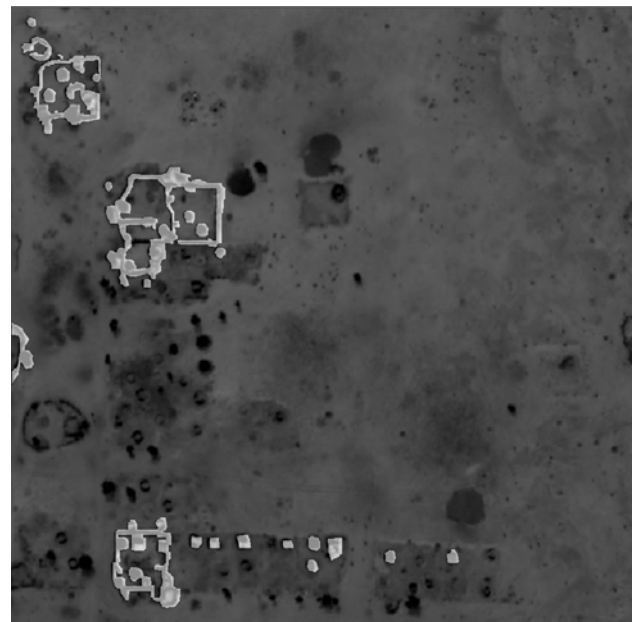


Figure 7. Manual digitized unchanged man-made structures and the subset of the Shangil village after destruction  
©Digital Globe 2006

The comparison with a manual digitized classification (based on figure 4) of the unchanged man-made structures (buildings, fences) shows (see figure 7), that the algorithm visualizes

nearly all unchanged buildings, but also some small areas with high texture values, that have changed (ruins and stone formations). However, it is easy to distinguish between destroyed and not destroyed structures.

Table 8 shows the overall results of the qualitative assessment respectively visual interpretation for the different methods and texture features. The table compares and assesses the change results of the different change detection methods (left column) in relation to the four texture images (upper row).

	<b>Con- trast</b>	<b>Correlation</b>	<b>IDM</b>	<b>Energy</b>
<b>Image-differencing</b>	-	-	-	-
<b>Image-ratio</b>	-	-	0	0
<b>Regression</b>	0	0	0	0
<b>PCA</b>	-	-	-	+

Table 8. Assessment of the texture based change detection result: Evaluation: „+“ = good visualization, „0“ = partly visualization and „-“ = bad visualization of changes

#### 4. CONCLUSIONS

A comparison of four different texture characteristics *contrast*, *correlation*, *inverse distance moment* (IDM) and *energy* that were used for four different change detection methods (image-differencing, image-ratioing, regression and PCA) shows that a combination of a bitemporal principal component analysis with the texture feature *energy* displays the best results for the visualization of change. Image of a village in the Darfur region before and after destruction were used for our study. However, the used test area was ideal to show the possibilities of texture-change analysis, because most of the buildings were completely destroyed and no texture was present on the locations of the destroyed buildings.

With the texture-based change detection approach, it is possible to visualize changed and unchanged settlement areas without the determination of thresholds. In our future work we will test this approach with other satellite images and airborne data and to show the transferability of this method.

#### REFERENCES

- AAAS, 2009. <http://shr.aaas.org/geotech/darfur/darfur.shtml>, Homepage of AAAS, accessed: October 2009.
- Amnesty International, 2009. <http://www.eyesondarfur.org>, Homepage of Amnesty International, accessed: October 2009.
- Bahrenberg, G., Giese, E. and Nipper, J., 1992. *Statistische Methoden in der Geographie: Multivariate Statistik* (Vol. 2). Vieweg+Teubner, Wiesbaden.
- Coppin, P., Jonckheere, I., Nackaerts, K., Muys, B. and Lambin, E., 2004. Review Article. Digital change detection methods in ecosystem monitoring a review. *International journal of remote sensing*, 25(9), pp. 1565–1596.
- Dai, X. and Khorram, S., 1999. Remotely Sensed Change Detection Based on Artificial Neural Networks. *Photogrammetric engineering and remote sensing*, 65(10), pp. 1187–1194.
- Ehlers, M. and D. Tomowski, 2008. On Segment Based Image Fusion, in: Blaschke, T., S. Lang and G. Hayes (Eds.), *Object-Based Image Analysis – Spatial Concepts for Knowledge-Driven Remote Sensing Applications*, Springer Lecture Notes in Geoinformation and Cartography, pp. 735–754.
- Foody, G. M., 2001. Monitoring the Magnitude of Land-Cover Change around the Southern Limits of the Sahara. *Photogrammetric Engineering and Remote Sensing*, 67(7), pp. 841–847.
- Haralick, R. M., Shanmugam, K. and Dinstein, I., 1973. Textural features for image classification. *IEEE Trans. Syst., Man, Cybern.*, (SMC-3), pp. 610–621.
- Haralick, R. M. and Shapiro, L. G., 1992. *Computer and Robot Vision - Volume 1*. Addison-Wesley, Reading.
- Im, J., Jensen, J. R. and Tullis, J. A., 2008. Object-based change detection using correlation image analysis and image segmentation. *International Journal of Remote Sensing*, 29(1–2), pp. 399–423.
- Jensen, J. R., 1986. *Introductory Digital Image Processing: A Remote Sensing Perspective*. Prentice-Hall, Englewood Cliffs, New Jersey.
- Jianyaa, G., Haiganga, S., Guoruia, M. and Qimingb, Z., 2008. A Review of multi-temporal remote sensing data change detection algorithms. In: The International Archives of the Photogrammetry, Remote Sensing and Spatial Information Sciences, Beijing, China, Vol. XXXVII, Part B7, pp. 757–762.
- Khorram, S., Biging, G. S., Chrisman, N. R., Colby, D. R., Congalton, R. G. and Dobson, J. E. et al., 1999. *Accuracy Assessment of Remote Sensing Derived Change Detection*. American Society for Photogrammetry and Remote Sensing, Bethesda.
- Kuenzel, W., 2007. Kartographie für den schnelleren Rettungseinsatz bei Naturkatastrophen: GIS bei den Vereinten Nationen und das Erdbeben in Pakistan. In E. Theile (Eds.), *Kartographische Schriften: Vol. 14. Kartographie - Ihnen werden wir's zeigen. Symposium 2007, 14 - 16. Mai 2007 Koenigslutter am Elm*. Kirschbaum, Bonn.
- Lehmann, T., Oberschelp, W., Pelikan, E. and Repges, R., 1997. *Bildverarbeitung für die Medizin: Grundlagen, Modelle, Methoden, Anwendungen*: Springer, Berlin.
- Lohmann, P., Hoffmann, P. and Müller, S., 2008. Updating GIS by object-based change detection. In J. Schiewe and M. Ehlers (Eds.), *gi-reports@igf - Geoinformatics paves the Highway to Digital Earth: On the occasion of the 60th birthday of Professor Manfred Ehlers* (Vol. 8, 1st ed., pp. 81–86). Osnabrueck.
- Lu, D., Mausel, P., Batistella, M. and Moran, E., 2005. Land-cover binary change detection methods for use in the moist tropical region of the Amazon: a comparative study. *International Journal of Remote Sensing*, 26(1), pp. 101–114.

- Lu, D., Mausel P., Brondízio E. and Moran E., 2003. Change detection techniques. *International Journal of Remote Sensing*, 25(12), pp. 2365–2407.
- Macleod, R. D. and Congalton, R. G., 1998. A Quantitative Comparison of Change-Detection Algorithms for Monitoring Eelgrass from Remotely Sensed Data. *Photogrammetric Engineering and Remote Sensing*, 64(3), pp. 207–216.
- Mas, J. –F., 1999. Monitoring land-cover changes: a comparison of change detection techniques. *International Journal of Remote Sensing*, 20(1), pp. 139–152.
- Mueller, B., 2000. Statistische Auswertungen von Untersuchungsergebnissen. In H. Barsch, K. Billwitz, and H.-R. Bork (Eds.), *Perthes Geographie Kolleg: Arbeitsmethoden in Physiogeographie und Geoökologie*. Gotha: Klett-Perthes, pp.407–449.
- Myint, S.W. , 2007. Urban Mapping with Geospatial Algorithms. In Q. Weng and D. A. Quattrochi (Eds.), *Urban Remote Sensing*. CRC Press, Boca Raton, pp.109–136.
- Nemmour, H. and Chibani, Y., 2006. Fuzzy neural network architecture for change detection in remotely sensed imagery. *International Journal of Remote Sensing*, 27(3-4), 705–717.
- Niemeyer, I. and Nussbaum, S., 2006. Automatisierte Detektion, Klassifizierung und Visualisierung von Veränderungen auf der Grundlage von Fernerkundungsdaten. In I. Niemeyer, A. Sroka and R. Wittenburg (Eds.), *Schriftenreihe des Institutes für Markscheidewesen und Geodäsie an der Technischen Universität Bergakademie Freiberg: Tagungsband des 7. Geokinematischen Tages vom 11. und 12. Mai 2006 in Freiberg*. Glueckauf, Essen, pp. 248–257.
- Nussbaum, S. and Menz, G., 2008. *Object-Based Image Analysis and Treaty Verification: New Approaches in Remote Sensing - Applied to Nuclear Facilities in Iran*. Springer Science+Business Media B.V., Dordrecht.
- Prakash, A. and Gupta, R. P., 1998. Land-use mapping and change detection in a coal mining area - a case study in the Jharia coalfield, India. *International Journal of Remote Sensing*, 19(3), pp. 391–410.
- Sali, E. and Wolfson, H., 1992. Texture classification in aerial photographs and Satellite data. *International Journal of Remote Sensing*, 13(18), pp. 3395–3408.
- Schowengerdt, R. A., 2007. *Remote Sensing: Models and methods for image processing* (3. ed.). Elsevier Academic Press, Amsterdam.
- Singh, A., 1989. Digital change detection techniques using remote-sensed data. *International Journal of Remote Sensing*, 10(10), pp. 989–1003.
- Steinnocher, K. T., 1997. Texturanalyse zur Detektion von Siedlungsgebieten in hochauflösenden panchromatischen Satellitenbilddaten. In *AGIT IX, 2.-4. Juli 1997, Salzburger Geographische Materialien*. Vol. 26, pp. 143–152.
- Tomowski, D., Ehlers, M., Michel, U. and Bohmann, G., 2006. *Objektorientierte Klassifikation von Siedlungsflächen durch multisensorale Fernerkundungsdaten*, gi-reports@igf, Vol. 3, University of Osnabrück, Osnabrück.
- Tomowski, D., Michel, U., Ehlers, M. and Bohmann, G., 2006. Siedlungsflächenklassifikation mittels objektorientierter Datenfusion durch multisensorale Fernerkundungsdaten. In U. Michel and K. Behncke (Eds.), *gi-reports@igf: Vol. 5. Veroeffentlichungen des AK Fernerkundung 2006*. University of Osnabrück, Osnabrück, pp.123–135.
- Yang, X. and Lo, C. P., 2000. Relative Radiometric Normalization Performance for Change Detection from Multi-Date Satellite Images. *Photogrammetric Engineering & Remote Sensing* 66(8), 967–980.

#### ACKNOWLEDGEMENTS

The presented work was done in the research project „Automated Change Detection methods for disaster applications“ at the Institute for Geoinformatics and Remote Sensing (IGF) at the University of Osnabrück.